

xGASS: The connection between angular momentum, mass and atomic gas fraction in nearby galaxies

Jennifer A. Hardwick,^{1,2*} Luca Cortese,^{1,2} Danail Obreschkow¹ and Barbara Catinella^{1,2}

¹International Centre for Radio Astronomy Research (ICRAR), University of Western Australia, Crawley, WA 6009, Australia

²Australian Research Council, Centre of Excellence for All Sky Astrophysics in 3 Dimensions (ASTRO 3D), Australia

Accepted 2022 August 26. Received 2022 August 17; in original form 2022 June 22

ABSTRACT

We use a sample of 559 disc galaxies extracted from the eXtended GALEX Arecibo SDSS Survey (xGASS) to study the connection between baryonic angular momentum, mass and atomic gas fraction in the local Universe. Baryonic angular momenta are determined by combining H_I and H₂ integrated profiles with two-dimensional stellar mass surface density profiles. In line with previous work, we confirm that specific angular momentum and atomic gas fraction are tightly correlated, but we find a larger scatter than previously observed. This is most likely due to the wider range of galaxy properties covered by our sample. We compare our findings with the predictions of the analytical stability model developed by Obreschkow et al. and find that, while the model provides a very good first-order approximation for the connection between baryonic angular momentum, mass and gas fraction, it does not fully match our data. Specifically, we find that at fixed baryonic mass, the dependence of specific angular momentum on gas fraction is significantly weaker, and at fixed gas fraction, the slope of the angular momentum vs. mass relation is shallower than what was predicted by the model. The reasons behind this tension remain unclear, but we speculate that multiple factors may simultaneously play a role, all related to the fact that the model is not able to encapsulate the full diversity of galaxy properties in our sample.

Key words: galaxies: disc – galaxies: evolution – galaxies: ISM – galaxies: kinematics and dynamics

1 INTRODUCTION

Understanding how galaxies grow in mass and structure across cosmic time, and if/how these processes can regulate the gas-star formation cycle, is a key step towards understanding how galaxies form and evolve. At least for disc galaxies, in our current theoretical framework, the growth of angular momentum (AM) of discs is tightly connected to the ability of galaxies to accrete gas and use it for star formation (e.g., Mo et al. 1998; Boissier & Prantzos 2000). As such, we expect some kind of correlation between the AM of discs and their cold gas fractions. While this link was initially suggested by early analytical studies, now it has been shown in both cosmological simulations and observations. For example, several independent studies have now shown that, at fixed mass, the spread in AM correlates with the amount of atomic gas available (e.g., Huang et al. 2012; Obreschkow et al. 2016; Lagos et al. 2017; Lutz et al. 2018; Stevens et al. 2018; Wang et al. 2019; Murugesan et al. 2019; Mancera Piña et al. 2021a; Kurapati et al. 2021; Hardwick et al. 2022).

The next step is clearly to move beyond simple correlations and understand whether or not they trace any underlying physical connection between AM and gas content. This task is far from being trivial. From an observational point of view, given that most of the observed galaxy properties are interconnected, identifying the potential physical drivers of scaling relations demands a very large

number statistics. In fact, only in this way can we look for trends after controlling for various galaxy properties (e.g., mass, morphology and environment). Unfortunately, as discussed below, we are still lacking information for both AM and gas content for a large enough sample to properly dissect the AM-mass-gas fraction plane, in the same way that has been done for other well-known scaling relations (Bernardi et al. 2003; Courteau et al. 2007; Saintonge & Catinella 2022). This is equally difficult from a theoretical point of view, as there is limited ability for cosmological simulations to trace multiple and interconnected physical processes, which makes it challenging to identify the dominant driver of scaling relations. This is where simpler analytical models can provide a complementary view to the problem, as they allow us to test whether or not a simple framework of galaxy evolution is able to reproduce our observed trends.

Intriguingly, in the last few years, the analytical approach has been extremely popular in our quest for understanding the potential physical link between AM and gas content. In particular, Obreschkow et al. (2016, hereafter O16) have put forward an analytical model showing how this correlation can be interpreted from a disc stability point of view (see also Romeo 2020 for an alternative approach). They relate the baryonic AM and mass of a galaxy to its atomic gas content by using the Toomre (1964) stability parameter. Specifically, they assume galaxies to be thin axisymmetric exponential discs, and calculate regions where gas is stable to collapse and could remain atomic, based on the galaxies baryonic AM. The total atomic gas fraction of a system is then obtained by integrating the gas mass in

* E-mail: jennifer.hardwick@icrar.org

these stable regions. Many previous works have shown that the **O16** model matches H α -selected disc galaxies in observations (Lutz et al. 2018; Murugesan et al. 2019; Džudžar et al. 2019; Murugesan et al. 2020; Li et al. 2020; Murugesan et al. 2021; Kurapati et al. 2021), and is qualitatively consistent with predictions from cosmological simulations (Wang et al. 2018; Stevens et al. 2018, 2019). This has been used as a strong support to the idea that AM is connected to the amount of atomic gas fraction in galaxies.

While promising, the agreement between observations and the **O16** model has so far been established primarily for pure discs, gas-rich galaxies, which may not be representative of the local galaxy population, particularly at stellar masses higher than $10^{10} M_{\odot}$ (e.g., Catinella et al. 2018; Cook et al. 2019). As such, it is important to extend previous analyses to samples spanning significantly larger ranges of morphologies and gas fractions.

In fact, recent work on the topic has started providing us with hints of a potential tension between observations and the **O16** model. Mancera Piña et al. (2021a,b) used a sample of 157 galaxies with resolved H α information to investigate the link between the scatter of the AM-mass relation (i.e., the Fall 1983 relation) and H α gas fraction. While they find a significant correlation between the two quantities, they were not able to match their finding with the **O16** model. In Hardwick et al. (2022, hereafter referred to as Paper 1) we investigated the stellar AM - mass relation for the largest representative sample of nearby galaxies with H α measurements to date (the extended GALEX Arcicibo SDSS survey; Catinella et al. 2018). Again, we found a strong correlation between H α gas fraction and stellar specific AM, but we show how this correlation becomes weaker for high mass galaxies with a photometric bulge component, potentially highlighting some deviations from the expectations for pure disc systems. However, to test these conclusions, it is critical to perform a careful comparison with the **O16** model that not only focuses on the stellar specific AM, but also considers the full baryonic AM of galaxies.

Thus, in this paper, we build on the work done in Paper 1 and investigate in detail whether or not the **O16** model can provide a quantitatively accurate representation of the correlation between AM, mass and gas fraction, over a large range of stellar masses and gas content.

This paper is set out as follows. In Section 2 we outline the sample used and summarise how these measurements were determined. In Section 3 we describe how we calculate baryonic mass and specific AM needed to investigate the **O16** relation. Section 4 gives the key results of this work on the **O16** relation and our empirical fit before discussing their implications in Section 5. We conclude and summarise our findings in Section 6.

2 SAMPLE

The extended GALEX Arcicibo SDSS Survey (xGASS; Catinella et al. 2010, 2018) has the most sensitive H α observations for a large representative sample in the local Universe, covering stellar masses between $10^9 M_{\odot}$ and $10^{11.5} M_{\odot}$ across the redshift range $0.01 < z < 0.05$. xGASS was selected from the Sloan Digital Sky Survey, Data Release 6 (SDSS DR6; Adelman-McCarthy et al. 2008) spectroscopic catalogue overlapping with the GALaxy Evolution Explorer (GALEX; Martin et al. 2005) sky footprint. H α masses and velocity widths were determined by taking observations with the 305m Arcicibo single-dish telescope. Each observation was taken until H α was detected or a gas fraction limit of 2% to 10% (depending on stellar mass) was reached.

In this work, we use the sub-sample of galaxies extracted from the xGASS survey that were detected in H α (not including any with possible H α confusion) and have inclinations greater than 30 degrees, for which stellar AM estimates have been determined in Paper 1. We refer the reader to this paper for details on the technique and here provide just a brief summary.

We calculated j_{\star} using spatially unresolved H α observations and reconstructed surface density profiles integrated out to 10 effective radii (R_e). Rotation curves were assumed to be flat with maximum rotational velocities equal to half the H α width (corrected for inclination) measured at 50% of the peak flux. In this paper, we focus on the AM of the disc only and restrict our sample to galaxies with a disc component as identified by 2D decompositions (Cook et al. 2019): 559 galaxies in total.

Molecular gas masses are taken from xCOLD GASS (extended CO Legacy Database for GASS; Saintonge et al. 2011, 2017). This database was created as a follow up of xGASS to determine molecular gas masses. CO (1-0) observations were taken on the IRAM 30m telescope for 45% of the xGASS galaxies (these were randomly selected). In our sub-sample, we have 248 galaxies that overlap with the xCOLD GASS data. Of these overlapping galaxies, 196 galaxies have a CO (1-0) detection which can be used to determine a molecular gas mass using a metallicity-dependent conversion function (Accurso et al. 2017), while the remaining 52 galaxies have upper limits (3σ). For galaxies that were not observed with xCOLD GASS, or only had upper limits, we used estimated molecular gas masses from star formation rates (SFRs) in our analysis (see Section 3.1).

Global SFRs and galaxy environment measures are taken from the analysis of Janowiecki et al. (2017). They determined SFRs by combining GALEX near-ultraviolet and WISE (Wright et al. 2010) mid-infrared photometry and galaxy environments from the Yang et al. (2007) group catalogues of SDSS. For reference, the star-forming main sequence (MS) for xGASS is presented in Catinella et al. (2018) and Janowiecki et al. (2020). To calculate the offset from the MS (ΔMS) for each galaxy, we take the difference between the MS (as is defined in Catinella et al. 2018) and the specific SFR (SFR/M_{\star}) of the galaxy, at its stellar mass.

3 METHODS

While in Paper 1 we focus on stellar AM, in order to fully investigate the physical connection between gas content and disc stability we need to quantify the total baryonic mass and baryonic AM of galaxies. Therefore, in this section, we describe how these quantities are derived for our sample.

3.1 Baryonic Mass

We assume that the baryonic component of disc galaxies can be fully represented by a combination of stars, atomic gas and molecular gas. We use molecular gas masses from xCOLD GASS, (this includes a helium contribution). Atomic gas is comprised of atomic hydrogen (H α , taken from xGASS) and helium (assumed to be 35% of the H α). We also assume that all the hydrogen and inferred helium are located in the disc. Using bulge-to-disc decompositions, the stellar mass of the disc component can be separated (for details see Cook et al. 2019 and Hardwick et al. 2022). Therefore, the baryonic mass of the disc is given as follows:

$$M_{\text{bar,D}} = M_{\star,D} + M_{\text{mol}} + 1.35M_{\text{HI}} \quad (1)$$

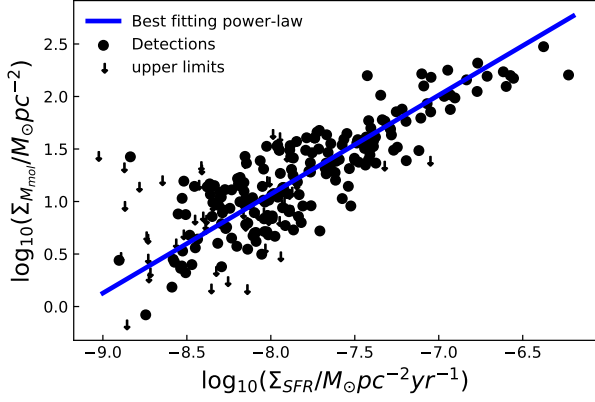


Figure 1. The inverted Kennicutt-Schmidt relation for the 251 galaxies in our sample with observations available from xCOLD GASS. Points are detections with downward arrows indicating non-detections at their 3σ upper limit. The best-fit power-law to the detections is shown as a thick blue line, with its formula given in Equation 2

where $M_{\star,D}$ is the stellar mass of the disc, M_{HI} is the mass of atomic hydrogen gas and M_{mol} is the mass of molecular gas.

Despite all our galaxies having HI and stellar masses, only 45% of our sample has molecular gas masses from xCOLD GASS. Therefore, the remaining 363 galaxies in our sample need their molecular gas mass estimated. We use the SFR surface density ($\Sigma_{SFR} = SFR/\pi R_e^2$) vs. molecular mass surface density ($\Sigma_{mol} = M_{mol}/\pi R_e^2$) relation (i.e., the inverted Kennicutt-Schmidt law, Kennicutt 1989; Schmidt 1959) to estimate molecular gas for the galaxies not observed or with only upper limits in xCOLD GASS. Here, R_e is the r-band half-light radius of the total galaxy. Figure 1 shows this relation for the subset of our sample observed with xCOLD GASS. For this sub-sample, the SFR and molecular gas surface densities are related by the following formula;

$$\log_{10}(\Sigma_{M_{mol}}/M_{\odot}\text{pc}^{-2}) = 0.94 \log_{10}(\Sigma_{SFR}/M_{\odot}\text{pc}^{-2}\text{yr}^{-1}) + 8.61 \quad (2)$$

which was determined by fitting a power-law (blue line) in HYPER-FIT¹ (Robotham & Obreschcow 2015) to the galaxies with H₂ detections. Using equation 2, we obtain molecular gas masses from SFRs for the galaxies where a CO detection is not available. For two of the galaxies in our sample, we do not have SFRs or H₂ detections (GASS123007 and GASS38198). For these, we determine the molecular gas mass by assuming that their HI-to-H₂ mass ratio is the average value observed in our sample (i.e., 20%). As H₂ contributes very little to both M_{bar} and j_{bar} , these assumptions do not affect our results.

3.2 Specific Angular Momentum of the Baryons

To calculate the baryonic specific AM of the disc ($j_{bar,D}$) we take the mass-weighted average of the specific AM of each component; stars, HI and molecular gas, as follows:

$$j_{bar,D} = \frac{j_{\star,D}M_{\star,D} + j_{mol}M_{mol} + 1.35j_{HI}M_{HI}}{M_{\star,D} + M_{mol} + 1.35M_{HI}}, \quad (3)$$

¹ This same code has been used to determine all the best fits in this paper.

where $j_{\star,D}$, j_{mol} and j_{HI} are the specific AM of the disc stars, molecular gas and HI, respectively. We use the values of $j_{\star,D}$ that are available from Paper 1.

We assume that j_{mol} is equal to $j_{\star,D}$. This is because it has been shown in works such as Bigiel & Blitz (2012) and Smith et al. (2016) that the surface density profile of the H₂ follows closely that of the stars. The specific AM is primarily set by the surface mass density distribution (assuming that the rotation curves are similar for both components), so it follows that the specific AM of the H₂ is the same as the stars.

To determine j_{HI} from spatially unresolved data, we proceed as follows. Firstly, we assume the HI surface density profile (Σ_{HI}) to be universal for all galaxies. This was shown to be a good approximation for the sample in Wang et al. (2016) when radii were normalised by the HI diameter. To determine the HI diameter we use the intrinsically tight HI mass to size relation from Wang et al. (2016):

$$\log_{10}(D_{HI}/\text{kpc}) = (0.506 \pm 0.003) \log_{10}(M_{HI}/M_{\odot}) - (3.293 \pm 0.009), \quad (4)$$

where D_{HI} is the diameter of the HI disc measured at a surface density of $\Sigma_{HI} = 1 M_{\odot}\text{pc}^{-2}$. We tested the reliability of this approach by also allowing for a variation in diameter consistent with 1σ above and below the relation. Accounting for the scatter in the HI mass-diameter relation changes j_{HI} by a mean difference of ± 0.06 dex. The Σ_{HI} profiles from Wang et al. (2016) are only given out to $1.3R_{HI}$, (where $R_{HI} = 0.5D_{HI}$), which for the majority of our galaxies (92% of the sample) is less than the extent used to estimate j_{\star} (i.e., $10R_e$). For consistency with all other quantities j_{HI} is also calculated within $10R_e$. To do so, we linearly extrapolate the universal Σ_{HI} profile (in log-log space). This extrapolation slightly increases the value of j_{HI} (less than 0.03 dex). Conversely, for the 46 galaxies, where $10R_e < 1.3R_{HI}$, j_{HI} is reduced by an average of 0.02 dex up to a maximum of 0.15 dex, when compared to j_{HI} calculated within $1.3R_{HI}$.

Lastly, we assume that the velocity profile is constant for all radii and given by the width of the HI emission line. This is the same assumption made in Paper 1 for calculating stellar specific AM. This assumption was tested in Paper 1 by comparing constant velocity profiles to the template rotation curves in Catinella et al. (2006), where we showed that the most extreme case of low-mass dwarf galaxies (i.e. $M_{\star} \approx 10^9 M_{\odot}$), had a maximum systematic offset in j of ~ 0.08 dex, while high-mass galaxies had less discrepancy (< 0.04 dex). Therefore, this assumption only introduces minor systematic effects which do not impact our result (for more details see Paper 1). We emphasise that, despite using a constant velocity profile, our approach does not rely on the approximation of $j \propto V_{max}R_e$ (Romanowsky & Fall 2012), and instead estimates j by directly integrating the AM profile obtained from the surface density profiles of each baryonic component. We found this to be a more accurate way to determine AM, as the Romanowsky & Fall (2012) approximation can overestimate a galaxies AM by up to 25% at low masses (e.g., Obreschcow & Glazebrook 2014; Bouché et al. 2021).

Once all of these assumptions are combined, we obtain j_{HI} . When comparing $j_{\star,D}$ and j_{HI} , on average j_{HI} is roughly twice the value of $j_{\star,D}$, although there is a considerable spread ($\sigma = 0.22$ dex). Note that this factor ~ 2 was also found in THINGS (Obreschcow & Glazebrook 2014) using resolved HI kinematic maps.

We reiterate that although we have outlined many assumptions in this subsection, these choices are not likely to affect our results. Although we assume that stars and gas share the same rotation curve (by using HI line widths to calculate AM for both), this does not

impact our results. Stellar rotation curves rise more slowly than cold gas ones due to asymmetric drift, so our estimates of $j_{\star,D}$ may be slightly overestimated. However, j_{bar} would not change considerably if $j_{\star,D}$ was altered slightly. In addition, assumptions made when calculating $j_{\star,D}$ were robustly tested in [Paper 1](#). As mentioned above, the assumptions involving j_{HI} have been tested, and even if these assumptions are altered, they do not affect the result significantly. In addition, the molecular mass is only a small component of our galaxies, such that excluding molecular material, only alters M_{bar} by 0.02 dex and j_{bar} by 0.01 dex on average. In summary, the typical uncertainty on our estimate of j_{bar} is 0.14 dex, which is dominated by the assumptions made on j_{HI} . This is comparable to the statistical error on M_{bar} , i.e., 0.11 dex.

4 RESULTS

In this section, we investigate the connection between j_{bar} , M_{bar} and atomic gas fractions.

4.1 Baryonic Fall Relation

As a first step, in [Figure 2](#) we show the baryonic Fall relation for galaxies in xGASS. The left panel shows the baryonic mass and specific AM for just the disc component ($M_{\text{bar},D}$ and $j_{\text{bar},D}$), while on the right we show the total (i.e., disc and bulge component; $M_{\text{bar},T}$ and $j_{\text{bar},T}$). Although the majority of the paper will focus on just the disc components, we also show the right panel to compare with previous works. The best-fit linear relation to our data is shown as a thin black line, with 1σ scatter shown by the dashed lines. The blue line shows the baryonic Fall relation found by [Murugesan et al. \(2020\)](#) and the magenta line is from [Mancera Piña et al. \(2021a\)](#), which both agree well with the best-fitting relation to our work. This is not a trivial result given the difference in samples and techniques used to determine this relation. Therefore, the agreement with previous work gives us confidence that our approach is solid and we can move forward in our analysis.

As for previous works, we suggest caution when interpreting the slopes of the baryonic Fall relation at face value, as our sample is not selected by baryonic mass. xGASS is selected to only include galaxies with stellar masses greater than $10^9 M_{\odot}$ with an oversampling at the high stellar mass end to increase statistics (as shown in [Paper 1](#) this distribution is conserved for our sub-sample). As such, the distribution in baryonic mass of our sample is not representative, with a deficiency of galaxies at lower baryonic masses. Below a baryonic mass of approximately $10^{9.8} M_{\odot}$, at fixed baryonic mass, our sample will preferentially miss galaxies at high gas fractions, whose stellar mass lies below the cut of $10^9 M_{\odot}$. In addition, we know from the results of works such as [Mancera Piña et al. \(2021a\)](#), see also [Paper 1](#)) that galaxies with higher gas fractions also have higher j_{bar} . Therefore, we would expect the Fall relation to be shallower for a sample that is uniformly distributed in baryonic mass. This echoes the conclusions of [Paper 1](#), which found that the sample used to determine a Fall relation will affect the slope obtained.

4.2 H I content predicted from local stability

[O16](#) developed a formalism to look at the connection between specific baryonic AM, baryonic mass and atomic gas. This resulted in a dimensionless effective stability parameter q ;

$$q \equiv \frac{j_{\text{bar},D} \sigma_{HI}}{G M_{\text{bar},D}}, \quad (5)$$

where $j_{\text{bar},D}$ is the baryonic specific AM of the disc component, σ_{HI} is the one-dimensional velocity dispersion of H I, G is the gravitational constant and $M_{\text{bar},D}$ is the baryonic mass of the disc component. We use $M_{\text{bar},D}$ and $j_{\text{bar},D}$ as defined in [sections 3.1 and 3.2](#) respectively. σ_{HI} is assumed to be a constant 10 km s^{-1} , which is set by the temperature of the warm neutral medium (following the assumption of [O16](#)). For a flat exponential disc, the q parameter relates to the expected fraction of atomic gas via;

$$f_{\text{atm}} = \min\{1, 2.5 q^{1.12}\}. \quad (6)$$

Here the fraction of atomic gas is defined as the fraction of disc baryonic mass in neutral atomic hydrogen and helium;

$$f_{\text{atm}} = \frac{1.35 M_{HI}}{M_{\text{bar},D}}. \quad (7)$$

This stability model assumes that any atomic gas that is unstable (following the [Toomre 1964](#) stability parameter Q) will collapse to form stars. As a consequence, if $f_{\text{atm}} > \min\{1, 2.5 q^{1.12}\}$, then the galaxy is over-saturated in H I and is bound to form stars quickly (i.e., within a giant molecular clouds free-fall time). However, in the opposite case ($f_{\text{atm}} < \min\{1, 2.5 q^{1.12}\}$) a galaxy will remain stable, with no self-regulating processes to alter its atomic gas fraction. Therefore, the [O16](#) relation (equation 6) can be thought of as an upper limit of the amount of atomic gas that a galaxy can hold (for further details of the models assumptions see [O16](#)).

[Figure 3](#) shows the relationship between the q stability parameter and f_{atm} . We compare our sample (grey) to the data presented in [O16](#) (coloured points) and their model (black line). The binned median of our data (thick blue line) shows good agreement with the theoretical relation shown in black, however, our data show a larger scatter. For our data the median 16th to 84th percentile is 0.52 dex, whereas it is 0.27 dex for the original [O16](#) data. This result does not depend on the method used to determine M_{mol} , as f_{atm} only weakly depends on the molecular gas mass, and is mostly constrained by the H I mass. The significant scatter observed for xGASS is an important result, as previous work have used the small observed scatter in the $f_{\text{atm}} - q$ relation to support a scenario in which q is the primary galaxy property physically connected to gas fraction (e.g., [Obreschkow et al. 2016](#); [Lutz et al. 2018](#); [Murugesan et al. 2019](#)). Instead, for our sample, the $f_{\text{atm}} - q$ relation shows a spread comparable to that of the well-known relation between gas fraction and $NUV - r$ colour (median 16th to 84th percentile 0.49 dex).

As mentioned above, the [O16](#) model predicts that galaxies will not lie above the relation for long, as their H I gas will be unstable and collapse to form stars. [O16](#) expect most galaxies to lie within 40% of the analytical relation given the approximate uncertainties of the model, with only 6 out of their 105 galaxies lying above this point. In our data, above this limit, we have roughly double the fraction (61/559) than found in [O16](#). To understand if this is simply due to issues with the data, we analysed the 61 outlier galaxies via the Tully-Fisher relation ([Tully & Fisher 1977](#)) and found that only 11 of them appear to have underestimated rotational velocities. Therefore, as this issue does not affect the rest of the population scattering above the theoretical line, it suggests that the larger scatter compared to what is seen in [O16](#) is not due to data quality but intrinsic to our sample.

Previous works have shown that the down-ward scatter of the $f_{\text{atm}} - q$ relation can be due to environmental effects removing the gas from the disc without affecting the stability parameter (e.g. [Li et al. 2020](#); [Cortese et al. 2021](#)). If we divide our sample into central ($N=432$) and satellites ($N=122$) according to the classification from the [Yang et al. \(2007\)](#) group catalogue, we find that even in our sample, at fixed q , satellites show a lower f_{atm} (0.2 dex on average)

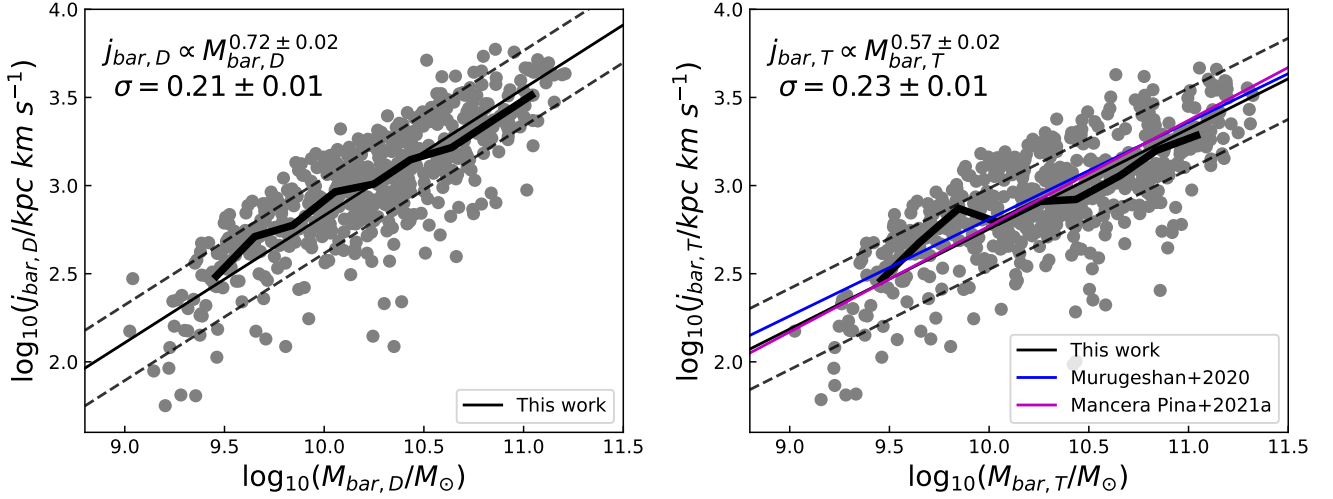


Figure 2. The baryonic Fall relation of the disc component (left) and the whole galaxy (i.e., disc plus bulge component; right). The best-fitting linear relation is shown as a thin black line, with the 1σ vertical scatter indicated by the dashed lines. The median in bins of baryonic mass (width = 0.2 dex) is shown as a thick black line (bins containing less than 10 galaxies are not shown). In the right panel, we compare to the work of [Murugesan et al. \(2020\)](#) in blue and [Mancera Piña et al. \(2021a\)](#) in magenta.

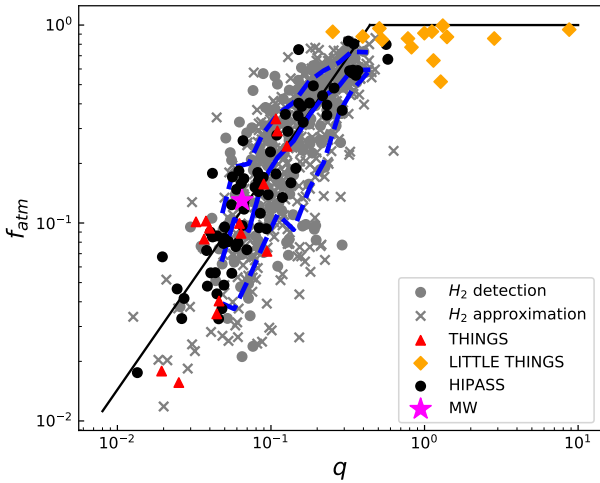


Figure 3. The distribution of our xGASS sample in the f_{atm} - q plane (grey symbols). Circles show galaxies with H_2 detections, while crosses are objects for which H_2 masses have been estimated from SFRs as discussed in Section 3. The blue lines show the median (solid) and 16th and 84th percentiles (dashed) for our sample, while the black line shows the theoretical relationship between q and f_{atm} given in Equation 6. The other symbols indicate the samples used in [O16](#) for their comparison with the model.

than central galaxies. This is intriguing, as xGASS includes less extreme density environments than the Virgo cluster analysed in [Li et al. \(2020\)](#). However, even if we focus on central galaxies alone, the scatter in the $f_{atm} - q$ relation remains substantial, with a median 16th to 84th percentile of 0.42 dex. This means that the large spread in f_{atm} at fixed q does not only trace environmentally-driven gas stripping.

To further understand the physical origin for this large scatter, we tested many potential galaxy parameters that could be correlated with

Parameter	Spearman Correlation Coefficient
ΔMS	$\rho_s = 0.43 \pm 0.04$
specific SFR	$\rho_s = 0.33 \pm 0.04$
Baryonic Mass	$\rho_s = 0.29 \pm 0.04$
H I Depletion time	$\rho_s = 0.25 \pm 0.04$
B/T	$\rho_s = -0.14 \pm 0.04$
Sersic index	$\rho_s = -0.11 \pm 0.04$

Table 1. The strength of correlation between Δf_{atm} (the vertical offset of our data from the [O16](#) model) and various integrated galaxy properties quantified via the Spearman correlation coefficient and its 1σ errors (determined from bootstrapping).

the vertical offset from the theoretical $f_{atm} - q$ relation, defined as follows;

$$\Delta f_{atm} = \log_{10}(f_{atm}) - \log_{10}(\min\{1, 2.5 q^{1.12}\}). \quad (8)$$

Namely, we investigated: the bulge-to-total mass ratio (B/T), Ser-sic index, H I depletion time (M_{HI}/SFR), baryonic mass ($M_{bar,D}$), specific SFR and the offset of galaxies from the star-forming main sequence (ΔMS , see Section 2). These parameters were chosen as they either related to morphology (which has been shown to relate to the scatter of the Fall relation; [Romanowsky & Fall 2012](#); [Cortese et al. 2016](#); [Hardwick et al. 2022](#)) or are an aspect of the model that we wanted to make sure was being encapsulated properly. We use the Spearman rank correlation coefficients (ρ_s) to quantify the correlation between each quantity and the offset from the theoretical line, as shown in Table 1 in descending order of correlation. We chose to use Spearman rank to measure the correlation as it does not make any assumptions on the type of correlation between the two quantities. The strongest correlation with Δf_{atm} is ΔMS , which is known to be strongly linked to a galaxy’s atomic gas reservoir (e.g. [Catinella et al. 2018](#); [Janowiecki et al. 2020](#); [Saintonge & Catinella 2022](#)). There is also a non-negligible correlation between Δf_{atm} and $M_{bar,D}$. This implies that the $f_{atm} - q$ plane may not provide the best representation for the link between AM and gas content in our data, and that xGASS galaxies may be better described by a model with different dependencies on f_{atm} and $M_{bar,D}$. Therefore, the next

step is to use a more empirical approach and look for the best way parameterise the correlation between $j_{\text{bar},D}$, $M_{\text{bar},D}$ and f_{atm} .

4.3 Empirical 3D fit to $j - M - f_{\text{atm}}$

By fitting a plane to specific AM, mass and gas fraction, we aim to quantify what functional form better describes our data and how this differs from the O16 model. We chose to fit two planes; one for the baryonic parameters ($j_{\text{bar},D}$, $M_{\text{bar},D}$ and f_{atm}) and one for stellar parameters ($j_{\star,D}$, $M_{\star,D}$ and $f_{\star,\text{atm}} = 1.35M_{\text{HI}}/M_{\star,D}$). Although the majority of this work is focused on baryonic parameters, we also chose to investigate this parameter space using just stellar properties as, a) the stellar parameters have been more extensively studied in the literature (e.g., Mancera Piña et al. 2021b; Hardwick et al. 2022) and b) they allow us to check if any of our conclusions are affected by the assumptions made to estimate the baryonic AM. We fit these 3-dimensional planes using the following formula;

$$\log_{10}(j_i / \text{kpc km s}^{-1}) = \alpha \log_{10}(M_i/M_{\odot}) + \beta \log_{10}(f_i) + \gamma \quad (9)$$

where i is either disc baryons or stars (\star). The best-fitting parameters to equation 9 are shown in Table 2. For comparison, when the O16 relation is converted into this formalism, the free parameters of equation 9 would be $\alpha = 1$, $\beta = 1/1.12 \approx 0.89$ and $\gamma = \log_{10}(G / [\text{kpc} (\text{km s}^{-1})^2 M_{\odot}^{-1}]) - (1/1.12) \log_{10}(2.5) - \log_{10}(\sigma / [\text{km s}^{-1}]) \approx -6.72$. Table 2 shows that, as hinted in the previous section, the best-fit parameters to our data are significantly different from those predicted by the O16 model. In particular, there is a slightly weaker dependence on the mass (α) term, and a significantly weaker dependence on the gas fraction (β) term, which is approximately half that expected by the O16 model. The empirical fit also has a smaller scatter (0.15 dex vertical scatter in j_{bar} , compared to 0.23 dex vertical scatter observed for our data in the O16 projection).

We obtain very similar results to that of Mancera Piña et al. (2021b) who, as mentioned in Section 1, also fit a 3D plane to baryonic AM, mass and atomic gas fraction. The coefficients of our planes are consistent within 3σ , despite their work focusing on a small sample ($N = 157$) of gas-rich disc galaxies. The only major difference between the results of this work and that of Mancera Piña et al. (2021b) was that they are very confident in their error analysis and quoted intrinsic scatter of their plane (which did not include measurement errors). Conversely, as we believe that we are not able to estimate proper errors for each individual galaxy in our sample, we chose to give σ which includes both measurement and intrinsic scatter of the plane. If we assume that our error estimates are correct, we find enticing evidence for nearly zero intrinsic scatter in our plane, i.e., a plane much tighter than what found in Mancera Piña et al. (2021b). However, as mentioned above, these errors are only approximations and we advice caution in over-interpreting this result.

Figure 4 shows the stellar (panel a) and baryonic (panel b) relations in the mass - AM plane. Projections of the best-fitting 3D relations from Table 2 are shown for fixed gas fractions as coloured lines. To easily compare, points are colour coded in the same way (i.e., by their gas fractions). The 2D best-fit Fall relation is shown as a thin black line (with the vertical 1σ scatter as black dashed lines). For comparison, Figure 5 shows the same baryonic Fall relation presented in 4b, but this time the lines of constant gas fraction correspond to the prediction from the O16 model. The comparison between Figure 4b and 5 helps visualising the differences between the O16 model and the best-fit empirical relation. Specifically, as already mentioned, the empirical relation has a weaker dependence on atomic gas fraction, which can be seen by the larger separation of the lines of

constant gas fraction in Figure 5. The weaker dependence on baryonic mass is also evident, as the lines at fixed gas fraction have a shallower slope than the O16 projection.

A possible issue with the results presented so far is that xGASS was selected to have a nearly flat stellar distribution (Catinella et al. 2018; Hardwick et al. 2022), and the oversampling of high mass galaxies may affect our best-fitting results. To test this, we also fit the empirical relation including weights for each galaxy. Following Catinella et al. (2018), these weights were calculated to recover the M_{\star} distribution of a volume-limited sample using the local stellar mass function as defined in Baldry et al. (2012). We find that, even after including the weights, our best-fit parameters are within error of the values presented in Table 2. Therefore, for simplicity, we only present the values obtained without the weights.

Interestingly, the scatter of the empirical relation still shows a weak correlation with ΔMS , with a Spearman rank correlation coefficient of $\rho_s = 0.25 \pm 0.05$. Thus, it is worth exploring whether such residual dependence needs to be included in our fit. We trialled fitting a 4D plane, with ΔMS as a fourth parameter and found that the dependence on f_{atm} and $M_{\text{bar},D}$ was largely unchanged when compared to the 3D plane, with a very small dependence (-0.08 ± 0.02) given to the ΔMS term. In addition to this, the standard deviation between the 4D and 3D fits was unchanged. We conclude that any third-order dependence on ΔMS is negligible or at least within the scatter of the 3D fit presented here.

The choice to use a planar fit for our empirical relation was motivated by the aim of keeping a similar approach to the one adopted by O16, but we also tested for non-linear trends in the residuals of the empirical fit, to see if this choice was sensible. There is a slight curvature in the residuals, when binned in f_{atm} , as is shown in Figure 6. This is a potential indication that the 3D planar fit may be too restrictive. However, the curvature is very weak and would likely not change the fit considerably if fit with a curved surface. Therefore, while we cannot exclude a curvature in the plane, our sample size is too small to justify the use of a 3D curved surface to parametrise the j_{bar} , M_{bar} , f_{atm} plane.

5 DISCUSSION

Our work shows that the O16 model provides a good first-order representation for the relation between gas fraction and AM. However, thanks to the larger dynamic range covered by xGASS compared to previous samples, we have been able to highlight where this analytical model breaks down (in a similar way to Mancera Piña et al. 2021b). Specifically, we show that the predicted slope of the baryonic mass - AM relation at fixed gas fraction is shallower than what is predicted by O16, with a significantly weaker dependence on gas fraction. This is most evident in Figure 7, where we directly compare the O16 model and our empirical best-fit relation to our data at fixed gas fraction. In the top row, our data (coloured points) follow a shallower relation than what is predicted by O16 (shaded region), with the largest deviation at lower gas fractions.

It is important to note that our findings are not a by-product of the methodology adopted to estimate j_{bar} . In fact, our main conclusions remain the same if we use stellar quantities alone (see left panel of Figure 4), showing that our results are not driven by assumptions made on j_{HI} or j_{mol} . Furthermore, the difference between the O16 model and our best-fit plane is also evident if we examine galaxies in different gas fraction bins separately (as shown in Figure 7), for which any systematic variation in the shape of the HI surface density profile should be further reduced (see Wang et al. 2016).

		α	β	γ	σ
This work	stellar	0.81 ± 0.02	0.38 ± 0.02	-5.06 ± 0.21	0.21 ± 0.01
	baryonic	0.80 ± 0.02	0.48 ± 0.02	-4.86 ± 0.16	0.15 ± 0.01
O16 model	baryonic	1	0.89	-6.72	

Table 2. Best-fitting parameters (from equation 9) for empirical fits (j - M - gas fraction) to either the stellar component (top row) or the baryonic component (middle row). For comparison, the bottom rows shows the equivalent coefficients for the O16 model.

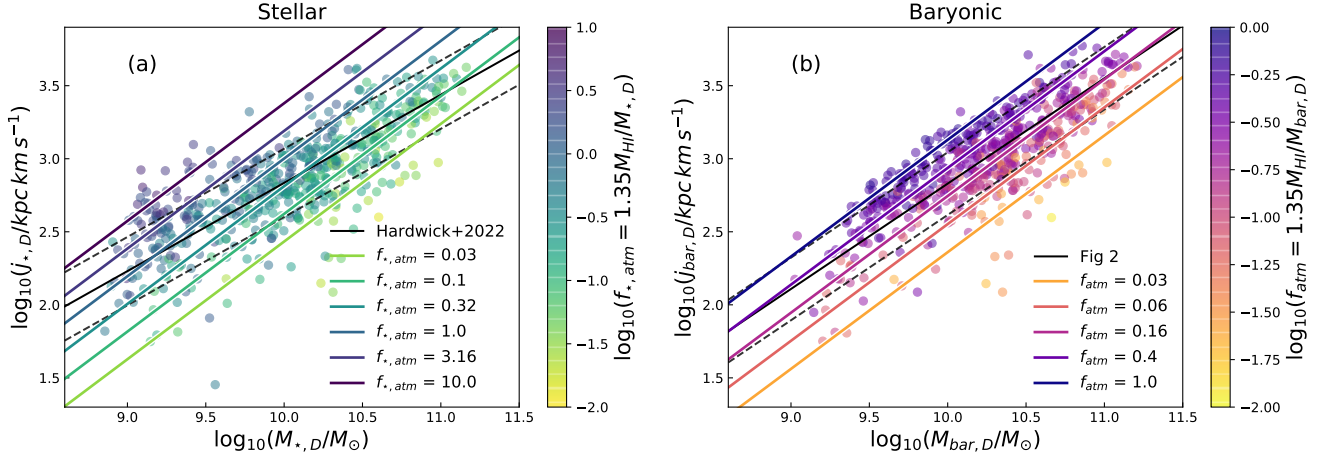


Figure 4. The stellar (a) and baryonic (b) 3D j - M - f_{atm} best-fit relations, in the j - M plane. The planes for fixed gas fractions are shown by the coloured lines. Our data points are also colour coded by the gas fraction to compare easily to the best-fits. The best-fitting 2D j - M relations are also shown as thin black lines (with dashed lines showing the 1σ vertical scatter).

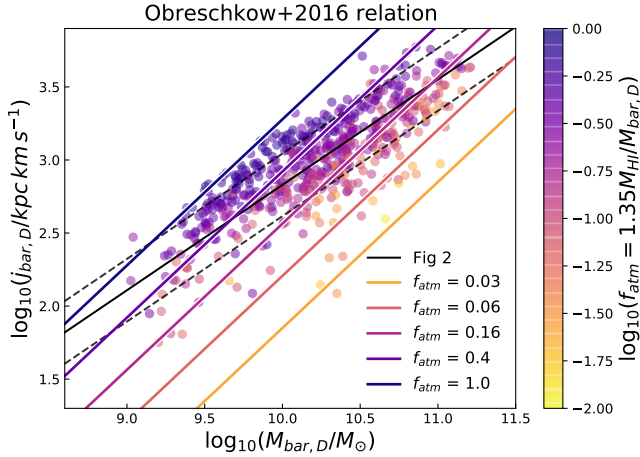


Figure 5. Same as Figure 4b, but now the coloured lines are projections from the O16 relation.

The inability of the O16 model to fully reproduce our data should not come as a surprise. This analytic model makes some simplistic assumptions, such as assuming atomic gas and stars are distinct spatially and galaxies are thin axially symmetric equilibrium discs with perfectly circular orbits, any of which could be causing the discrepancies between the model and our sample.

A similar analytical model has been recently put forward by Romeo (2020), which uses stability arguments to develop scaling relations involving AM. Their model treats each galaxy component (stars, atomic and molecular gas) separately, with each component regulating its own stability, leading to the expression $j_i \sigma_i / (GM_i) \approx 1$

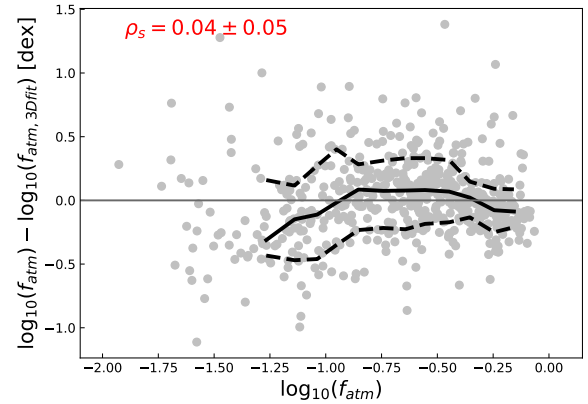


Figure 6. Vertical offset between the f_{atm} measured and that predicted by the empirical plane against f_{atm} . The black thick line shows the median in bins of f_{atm} , with each bin having a width of 0.1 dex and bins containing less than 10 galaxies not shown. Dashed lines show 16th and 84th percentiles of those bins.

(where i denotes either stars, atomic or molecular gas), which is then used to investigate the scaling relation between AM and gas or stellar mass fraction. We tested the prediction of the Romeo (2020) model on our sample focusing on atomic gas fraction, and found that our data disagree with the model. As with the disagreement with O16, our data prefer a model with a weaker dependence on gas fraction than the Romeo (2020) model predicts. This is also consistent with the recent work of Mancera Piña et al. (2021b), who found that the Romeo (2020) model was not able to reproduce their data either.

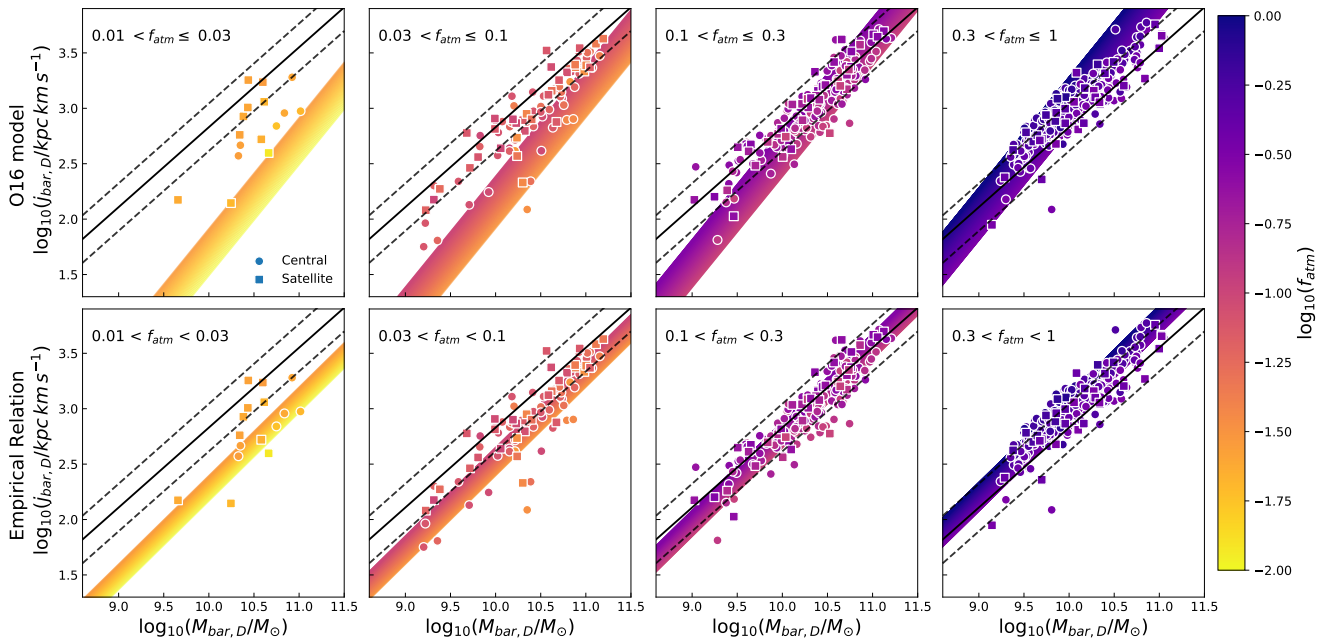


Figure 7. Comparison between the **O16** model (top row) and our best-fitting empirical relation (bottom row) in bins of gas fraction. Points are the same in both rows, showing our centrals (circles) and satellite galaxies (squares) colour-coded by their atomic gas fraction. Each column is an even log-spaced bin in gas fraction. The points are comparable to the coloured regions, which show the prediction from either the **O16** model or empirical relation for the given gas fraction bin. Overlaid in black for comparison are the best fitting 2D $j_{\text{bar}}-M_{\text{bar}}$ relation from Figure 2.

We can therefore go back and focus on the **O16** model. Before proposing any new changes, it is first important to remember that, as discussed in Section 4.2, the **O16** model does not predict a best-fitting scaling relation, but more simply identifies the parameter space in the $f_{\text{atm}} - q$ plane in which galaxies with stable HI discs should exist. Galaxies that have too much HI to be stable (i.e., lying above the model) will start rapidly forming stars causing the galaxy to drop down onto the model. No such self-regulation is expected below the model, where there is less HI than can be supported by the stability of the disc. This HI depletion can be easily achieved by many processes such as environmental processes, outflows, etc. Therefore, galaxies are not necessarily expected to be normally distributed around this model and instead preferentially scatter below the relation. As such a best-fit to a sample of galaxies that obeys the **O16** model will most likely be offset below the **O16** model. If we assume that processes that cause galaxies to scatter below the relation affect all masses equally, then this best-fit would have the same dependence on M_{bar} and f_{atm} as the **O16** model. However, as shown clearly in Figure 4 and 7, the best-fit empirical model has a different slope, implying a weaker dependence on baryonic mass and gas fraction than predicted. We briefly discuss if any processes could cause these changes.

One key assumption made in the **O16** model is that galaxies live in isolation. As discussed in Section 4.2, environment plays a role in the scatter around the **O16** relation, and can also introduce a mass dependence due to environmental processes being more efficient in low mass galaxies. However, this is unlikely to be the main driver of the deviations, as xGASS does not include galaxies in large cluster environments with the majority of the galaxies in our sample being central/ field galaxies. Even when we do exclude satellite galaxies from our sample, we still see a disparity between these galaxies and the **O16** model. Major mergers are also unlikely to be causing this

discrepancy, primarily because these are quite rare in the xGASS volume and confused galaxies (including close pairs and merging systems) were excluded from the sample.

The fact that galaxies are not isolated also implies that processes such as smooth gas inflows and outflows (and feedback in general) can play an important role in driving the deviations from the **O16** model. The effect of these is quite challenging to predict analytically. However, it is possible that feedback could impact the connection between gas fraction and q by affecting one or more of the key physical quantities at the basis of the **O16** model: i.e., gas content, AM and velocity dispersion.

Lastly, the modelling of the 3D structure of galaxies itself most likely harbours some of the limitations of the model. Local instabilities caused by spiral arms (e.g. Goldreich & Lynden-Bell 1965; Toomre 1977; Dobbs & Baba 2014), as well as the presence of a significant photometric bulge component in more than half of xGASS galaxies, makes our sample clearly deviating from the simple assumption of axis-symmetric thin discs made in the **O16** model. All this can easily make the assumption of constant HI velocity dispersion incorrect. In fact, it has been shown that the HI velocity dispersion radial profiles of nearby galaxies are not constant and that even the average value across the disc varies from galaxy to galaxy (e.g. Bacchini et al. 2019). In addition, if the change in σ_{HI} correlates with either baryonic mass or gas fraction, it may be even easier to reconcile the tension between our data and the **O16** model. Unfortunately, observational constraints on the variation of σ_{HI} with galaxy properties are still missing. However, this is an intriguing scenario which could address the issues emerged in this analysis without major changes to the overall physical framework of the **O16** model.

Admittedly, what we discussed so far is primarily speculation, but it is likely that more than one of the issues described above are driving

the differences between O16 and our data. This is because, as illustrated in Figure 7, the tension between our data and the O16 model are present even in the high gas fraction, disc-dominated regime for which this model has been calibrated, and then extends to more gas-poor disc plus bulge systems for which the assumptions of the O16 model naturally break. This highlights how understanding the physical drivers for the correlation between mass, AM and gas fraction is clearly a complex and multi-dimensional problem. The next step towards the solution of this problem may no longer come from a more elaborate analytical model, but instead from investigating this problem in a self-consistent cosmological framework. This will be our next step towards fully understanding the connection between AM and gas fraction and the origin of the weaker-than-expected correlation between these properties observed in the xGASS sample.

6 SUMMARY AND CONCLUSIONS

In this work, we have used a representative sample of galaxies in the local Universe with $10^9 < M_*/M_\odot < 10^{11.5}$ to investigate the connection between baryonic mass, specific AM and atomic gas fraction. We primarily focus on the comparison of our data with the predictions of the O16 stability model.

We show that, as a first-order approximation, the O16 model agrees well with our sample. However, when a full analysis is conducted, we see that our data show a slightly weaker dependence on baryonic mass, and half the dependence on atomic gas fraction than what suggested by the O16 model. This implies that the physical connection between AM and gas fraction may be weaker than claimed in previous works, and suggests that some of the assumptions made in the O16 model are not a good representation of the diversity of our data. While we speculate that part of this tension may be due to galaxy-to-galaxy variations, it is likely that multiple factors (e.g., internal galaxy properties and environmental effects) are simultaneously responsible for the weaker correlation between AM and gas fraction. In future work, we plan to further expand this analysis by performing a detailed study of cosmological simulations with the aim of gaining more insights into the exact cause of the discrepancy between our data and the O16 model.

ACKNOWLEDGEMENTS

We thank the anonymous referee for their comments which improved the clarity of our manuscript. JAH and LC acknowledge support from the Australian Research Council (FT180100066). Parts of this research were conducted by the Australian Research Council Centre of Excellence for All Sky Astrophysics in 3 Dimensions (ASTRO 3D), through project number CE170100013. DO is a recipient of an Australian Research Council Future Fellowship (FT190100083), funded by the Australian Government.

DATA AVAILABILITY

The data used in this work are publicly available at xgass.icrar.org/data.html.

REFERENCES

Accurso G., et al., 2017, *Monthly Notices of the Royal Astronomical Society*

- Adelman-McCarthy J. K., et al., 2008, *The Astrophysical Journal Supplement Series*, 175, 297
- Bacchini C., Fraternali F., Iorio G., Pezzulli G., 2019, *Astronomy and Astrophysics*, 622, A64
- Baldry I. K., et al., 2012, *Monthly Notices of the Royal Astronomical Society*, 421, 621
- Bernardi M., et al., 2003, *The Astronomical Journal*, 125, 1849
- Bigiel F., Blitz L., 2012, *The Astrophysical Journal*, 756, 183
- Boissier S., Prantzos N., 2000, *Monthly Notices of the Royal Astronomical Society*, 312, 398
- Bouché N. F., et al., 2021, *A&A*, 654, A49
- Catinella B., Giovanelli R., Haynes M. P., 2006, *The Astrophysical Journal*, 640, 751
- Catinella B., et al., 2010, *Monthly Notices of the Royal Astronomical Society*, 403, 683
- Catinella B., et al., 2018, *Monthly Notices of the Royal Astronomical Society*, 476, 875
- Cook R. H. W., Cortese L., Catinella B., Robotham A., 2019, *Monthly Notices of the Royal Astronomical Society*, 490, 4060
- Cortese L., et al., 2016, *Monthly Notices of the Royal Astronomical Society*, 463, 170
- Cortese L., Catinella B., Smith R., 2021, *Publications of the Astronomical Society of Australia*, 38, e035
- Courteau S., Dutton A. A., van den Bosch F. C., MacArthur L. A., Dekel A., McIntosh D. H., Dale D. A., 2007, *The Astrophysical Journal*, 671, 203
- Dobbs C., Baba J., 2014, *Publications of the Astronomical Society of Australia*, 31, e035
- Džudžar R., et al., 2019, *Monthly Notices of the Royal Astronomical Society*, 483, 5409
- Fall S. M., 1983, in *Internal Kinematics and Dynamics of Galaxies*. pp 391–398, <http://adsabs.harvard.edu/abs/1983IAUS...100..391F>
- Goldreich P., Lynden-Bell D., 1965, *Monthly Notices of the Royal Astronomical Society*, 130, 125
- Hardwick J. A., Cortese L., Obreschkow D., Catinella B., Cook R. H. W., 2022, *Monthly Notices of the Royal Astronomical Society*, 509, 3751
- Huang S., Haynes M. P., Giovanelli R., Brinchmann J., 2012, *The Astrophysical Journal*, 756, 113
- Janowiecki S., Catinella B., Cortese L., Saintonge A., Brown T., Wang J., 2017, *Monthly Notices of the Royal Astronomical Society*, 466, 4795
- Janowiecki S., Catinella B., Cortese L., Saintonge A., Wang J., 2020, *Monthly Notices of the Royal Astronomical Society*, 493, 1982
- Kennicutt Robert C. J., 1989, *ApJ*, 344, 685
- Kurapati S., Chengalur J. N., Verheijen M. A. W., 2021, *Monthly Notices of the Royal Astronomical Society*, 507, 565
- Lagos C. d. P., Theuns T., Stevens A. R. H., Cortese L., Padilla N. D., Davis T. A., Contreras S., Croton D., 2017, *Monthly Notices of the Royal Astronomical Society*, 464, 3850
- Li J., Obreschkow D., Lagos C., Cortese L., Welker C., Džudžar R., 2020, *Monthly Notices of the Royal Astronomical Society*, 493, 5024
- Lutz K. A., et al., 2018, *Monthly Notices of the Royal Astronomical Society*, 476, 3744
- Mancera Piña P. E., Posti L., Fraternali F., Adams E. A. K., Oosterloo T., 2021a, *Astronomy & Astrophysics*, 647, A76
- Mancera Piña P. E., Posti L., Pezzulli G., Fraternali F., Fall S. M., Oosterloo T., Adams E. A. K., 2021b, *Astronomy & Astrophysics*, 651, L15
- Martin D. C., et al., 2005, *The Astrophysical Journal*, 619, L1
- Mo H. J., Mao S., White S. D. M., 1998, *Monthly Notices of the Royal Astronomical Society*, 295, 319
- Murugesan C., Kilborn V., Obreschkow D., Glazebrook K., Lutz K., Džudžar R., Dénes H., 2019, *Monthly Notices of the Royal Astronomical Society*, 483, 2398
- Murugesan C., Kilborn V., Jarrett T., Wong O. I., Obreschkow D., Glazebrook K., Cluver M. E., Fluke C. J., 2020, *Monthly Notices of the Royal Astronomical Society*, 496, 2516
- Murugesan C., et al., 2021, *Monthly Notices of the Royal Astronomical Society*, 507, 2949
- Obreschkow D., Glazebrook K., 2014, *The Astrophysical Journal*, 784, 26
- Obreschkow D., Glazebrook K., Kilborn V., Lutz K., 2016, *The Astrophysical*

- [Journal Letters](#), 824, L26
- Robotham A. S. G., Obreschkow D., 2015, [Publications of the Astronomical Society of Australia](#), 32, e033
- Romanowsky A. J., Fall S. M., 2012, [The Astrophysical Journal Supplement Series](#), 203, 17
- Romeo A. B., 2020, [Monthly Notices of the Royal Astronomical Society](#), 491, 4843
- Saintonge A., Catinella B., 2022, [Annual Review of Astronomy and Astrophysics](#), 60
- Saintonge A., et al., 2011, [Monthly Notices of the Royal Astronomical Society](#), 415, 32
- Saintonge A., et al., 2017, [The Astrophysical Journal Supplement Series](#), 233, 22
- Schmidt M., 1959, [ApJ](#), 129, 243
- Smith M. W. L., et al., 2016, [Monthly Notices of the Royal Astronomical Society](#), 462, 331
- Stevens A. R. H., Lagos C. d. P., Obreschkow D., Sinha M., 2018, [Monthly Notices of the Royal Astronomical Society](#), 481, 5543
- Stevens A. R. H., et al., 2019, [Monthly Notices of the Royal Astronomical Society](#), 483, 5334
- Toomre A., 1964, [The Astrophysical Journal](#), 139, 1217
- Toomre A., 1977, In: [Annual review of astronomy and astrophysics. Volume 15. \(A78-16576 04-90\)](#) Palo Alto, Calif., [Annual Reviews, Inc.](#), 1977, p. 437-478. [NSF-supported research.](#), 15, 437
- Tully R. B., Fisher J. R., 1977, [Astronomy and Astrophysics](#), 54, 661
- Wang J., Koribalski B. S., Serra P., van der Hulst T., Roychowdhury S., Kamphuis P., Chengalur J. N., 2016, [Monthly Notices of the Royal Astronomical Society](#), 460, 2143
- Wang L., et al., 2018, [The Astrophysical Journal](#), 868, 93
- Wang L., et al., 2019, [Monthly Notices of the Royal Astronomical Society](#), 482, 5477
- Wright E. L., et al., 2010, [The Astronomical Journal](#), 140, 1868
- Yang X., Mo H. J., van den Bosch F. C., Pasquali A., Li C., Barden M., 2007, [The Astrophysical Journal](#), 671, 153

This paper has been typeset from a $\text{\TeX}/\text{\LaTeX}$ file prepared by the author.